

## FERROELECTRICITY AND STRUCTURAL PHASE TRANSITIONS IN A HEXAGONAL $ABX_3$ -TYPE ANTIFERROMAGNETIC COMPOUND: $\text{KNiCl}_3$

Ken-ichi MACHIDA, Toshiharu MITSUI<sup>1</sup>, Tetsuya KATO and Katsunori IIO

*Department of Physics, Faculty of Science,*

*Tokyo Institute of Technology, Oh-okayama, Meguro-ku, Tokyo 152*

<sup>1</sup> *Department of Physics, Faculty of Pharmaceutical Science, Teikyo University,  
Sagamiko-cho, Tsukui-gun, Kanagawa 199-01*

(Received 1 February 1994 by H Kamimura)

Dielectric properties of a hexagonal  $ABX_3$ -type antiferromagnet  $\text{KNiCl}_3$  are studied by measuring dielectric constants and observing  $D - E$  hysteresis loops. Dielectric anomalies indicating structural phase transitions are found exclusively along the  $c$ -axis at 274 K, 285 K, 561 K and 762 K. Ferroelectric  $D - E$  hysteresis loops are observed in the phase above 274 K, though the  $D - E$  loop cannot be observed at temperatures higher than 600 K owing to enhancement of electric conductivity of this compound. Within the observed temperature range, the spontaneous polarization  $P_s$  as a function of temperature behaves in a manner wherein as temperature is raised,  $P_s$  appears suddenly at 274 K, decreases gradually towards 285 K after substantial growth and then monotonically increases up to the phase above 561 K. The magnitudes of  $P_s$  at 274.5 K and 533.0 K are estimated as  $0.048 \mu\text{C}/\text{cm}^2$  and  $0.871 \mu\text{C}/\text{cm}^2$ , respectively. Such behavior of  $P_s$  is attributed to a possible ferroelectric alignment of sublattice polarizations inherent to the crystal structure with the space group  $P6_3cm$ .

### § 1 INTRODUCTION

Potassium nickel trichloride  $\text{KNiCl}_3$  is one of a series of hexagonal  $ABX_3$ -type magnetic systems, such like  $\text{CsNiCl}_3$ ,  $\text{CsMnBr}_3$  and  $\text{CsMnI}_3$ , which have attracted considerable attention for their low-dimensional magnetic properties and magnetic ordering processes on triangular lattices.<sup>1)-3)</sup> The dominant characteristics of these crystals are the presence of linear chains of face-sharing octahedra  $BX_6$  along the  $c$ -axis, where magnetic  $B$  ions compose triangular lattice nets. Among them,  $\text{KNiCl}_3$  has been known to undergo structural phase transitions from the prototype  $\text{CsNiCl}_3$ -structure with the space group  $D_{6h}^4-P6_3/mmc$  to lower symmetry phases successively at 250 K, 561 K and 762 K.<sup>4)</sup> The space group of the room-temperature structure was identified with  $C_{6v}^3-P6_3cm$  being polar, where the unit cell is described by enlarging that of  $\text{CsNiCl}_3$  to  $\sqrt{3}a$ ,  $\sqrt{3}a$  and  $c$ .<sup>5),6)</sup> The lattice constants  $\sqrt{3}a$  and  $c$  were determined as  $11.795 \text{ \AA}$  and  $5.926 \text{ \AA}$ , respectively (Fig 1). On the basis of group theory, Mañes and co-workers proved that the room-temperature structure of  $\text{KNiCl}_3$  is attributed to the condensation of the  $K_4$ -,  $K_1$ - and  $A_{2u}$ -lattice vibrational modes of the prototype  $\text{CsNiCl}_3$  structure.<sup>7),8)</sup> In particular, the  $K_4$ -mode representing the lattice distortion in which one of three  $\text{NiCl}_3$ -chains

shifts upward along the  $c$ -axis and two of them downward makes a major contribution to the displacements of ions of the room-temperature structure from the prototype lattice. Moreover, they pointed out that spontaneous polarization is induced by the condensation of the  $A_{2u}$ -mode which describes relative displacements of three different ionic groups along the  $c$ -axis.

On the other hand,  $\text{KNiCl}_3$  undergoes an antiferromagnetic phase transition at  $T_N = 8.2 \text{ K}$ , where ordered spin moments are confined within the  $c$ -plane.<sup>2)</sup> Antiferromagnetic ordering on the triangular lattice has an intrinsic instability due to spin frustration. If three equivalent nearest-neighbor antiferromagnetic couplings between magnetic ions on a triangular net split into different couplings owing to lattice distortions, spin ordering possibly becomes successive. Since  $\text{KNiCl}_3$  has a slightly distorted triangular lattice, the magnetic phase transition has to be reexamined together with elucidation of the crystal structure of the respective phases.

From these viewpoints, we have investigated the dielectric properties of  $\text{KNiCl}_3$  over a wide temperature range from 230 K to 780 K. As a result, the transition at 250 K reported previously by the present authors' group must be revised as successive transitions at 274 K and 285 K, we will designate the four transition points at 762 K, 561 K, 285 K and 274 K  $T_1$ ,  $T_2$ ,  $T_3$  and  $T_4$  in order

of decreasing temperature, respectively, and call the five crystalline states phases-I ( $T_1 \leq T$ ), -II ( $T_2 \leq T \leq T_1$ ), -III ( $T_3 \leq T \leq T_2$ ), -IV ( $T_4 \leq T \leq T_3$ ) and -V ( $T \leq T_4$ ). Furthermore,  $\text{KNiCl}_3$  was found to exhibit ferroelectricity along the  $c$ -axis at phases-II, -III and -IV. Therefore, the actual scenario of successive phase transitions of  $\text{KNiCl}_3$  may be more complicated than the theoretical prediction.

$\text{RbMnBr}_3$ <sup>9)</sup> and  $\text{RbFeBr}_3$ <sup>10)</sup> are examples of compounds belonging to the  $\text{KNiCl}_3$  family having the crystal structure of  $P6_3cm$  in some temperature range. In particular,  $\text{RbMnBr}_3$  has the same sequence of successive structural transitions as  $\text{KNiCl}_3$ . We have also succeeded in observing ferroelectric  $D-E$  hysteresis loops for  $\text{RbMnBr}_3$  and  $\text{RbFeBr}_3$ . Thus, it may be appropriate to state that the  $\text{KNiCl}_3$  family exhibits ferroelectricity together with magnetism. In this paper the ferroelectric and structural phase transitions in  $\text{KNiCl}_3$  are reported. Details for the other two compounds will be presented in separate papers<sup>11),12)</sup>

## § 2 EXPERIMENTS

Single crystals of  $\text{KNiCl}_3$  were grown by the Bridgman method from the melt of equimolar amounts of  $\text{KCl}$  and  $\text{NiCl}_2$ . Details of the growth conditions on growing crystals were as reported in ref 5. Samples used for all measurements were as-grown crystals, where specimens for the dielectric constant parallel to the  $c$ -axis,  $\epsilon_c$ , and that perpendicular to the  $c$ -axis,  $\epsilon_a$ , are cut into slabs with (001) faces and cleavage (11 $\bar{2}$ 0) faces, respectively. The sizes of the  $c$ - and the  $ac$ -slabs were about 4mm<sup>2</sup> and 10mm<sup>2</sup> in area, and 2.5mm and 0.5mm in thickness, respectively. In the high-temperature region above room temperature, gold electrodes were evaporated on the sample faces, and silver wires were attached with silver paste for avoiding sinking of silver

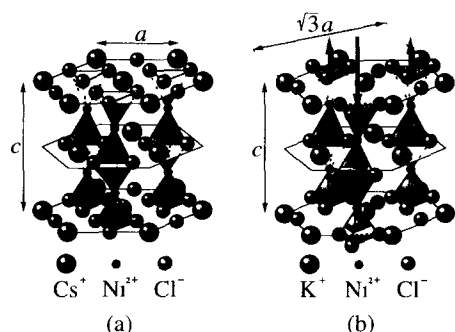


Fig 1 Crystal structures of (a)  $\text{CsNiCl}_3$  with the space group  $P6_3/mmc$ , (b)  $\text{KNiCl}_3$  with the space group  $P6_3cm$  at room temperature. In this figure the structure induced by condensation of only the  $K_4$ -mode is shown. The characteristic of these structure is to involve linear chains of face-sharing octahedra  $BX_6$  along the  $c$ -axis.

electrodes into samples, whereas silver paste was painted on the specimens as electrodes in the low-temperature region. Dielectric constants were measured at 1MHz with a YHP-4192A automatic impedance analyzer of which a  $c$  fields applied to the samples were about 4 V/cm. The heating and cooling rates were 2 K/min and 1 K/min, respectively. Temperatures are determined within  $\pm 0.5$  K above room temperature and  $\pm 0.1$  K below in the present study.  $D-E$  hysteresis loop observations were performed at 50Hz by means of a Sawyer-Tower circuit and the maximum value of the applied field was about 1.1 kV/cm.

## § 3 RESULTS

Figure 2 (a) shows the real parts of the complex dielectric constants,  $\epsilon_c$  and  $\epsilon_a$ , as functions of temperature in the range from 250 K to 300 K in heating and cooling runs, respectively. Anomalies associated with the structural phase transitions were observed only for  $\epsilon_c$  and were located at 274 K ( $= T_4$ ) and 285 K ( $= T_3$ ). In phase-IV, the increase of  $\epsilon_c$  accompanied a slight increase of the imaginary part of the dielectric constant  $\epsilon_c'$  due to electric conductivity. Around  $T_4$  there was a clear thermal hysteresis of about 4 K, but at  $T_3$  no hysteresis was observed. Therefore, the transitions at  $T_4$  and  $T_3$  are first- and second-order ones, respectively. Moreover, it was confirmed that dielectric constant increases with decreasing frequency.  $D-E$  hysteresis loops in the direc-

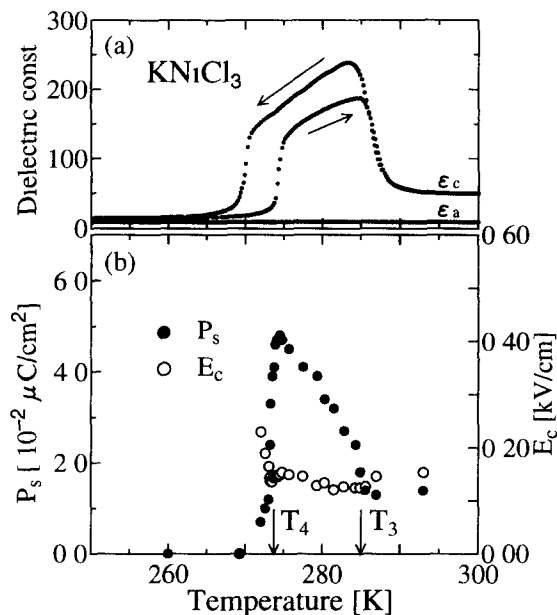


Fig 2 (a) Temperature dependence of dielectric constants  $\epsilon_c$  and  $\epsilon_a$  measured in cooling and heating runs at 1MHz below room temperature. (b) Spontaneous polarization and coercive field as functions of temperature in a heating run.

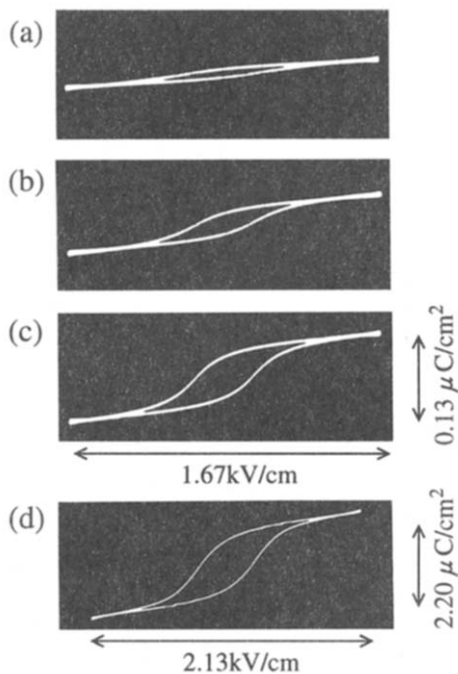


Fig 3 Ferroelectric 50Hz  $D - E$  hysteresis loops along the  $c$ -axis at (a) 272.6 K, (b) 273.2 K, (c) 274.5 K, (d) 533.0 K. The spontaneous polarizations and the coercive fields are (a) 0.010  $\mu\text{C}/\text{cm}^2$ , 0.190 kV/cm, (b) 0.024  $\mu\text{C}/\text{cm}^2$ , 0.144 kV/cm, (c) 0.048  $\mu\text{C}/\text{cm}^2$ , 0.150 kV/cm, (d) 0.871  $\mu\text{C}/\text{cm}^2$ , 0.196 kV/cm, respectively

tion along the  $c$ -axis were observed clearly in phases-III and -IV, but no hysteresis loops were observed for the  $ac$ -plate specimens. Photographs around  $T_4$  on heating are shown in Fig 3 (a), (b) and (c), where the saturation of these loops seems to be sufficient. The spontaneous polarization  $P_s$  at 274.5 K estimated by extrapolating the saturated portion of this loop with a straight line is about 0.048  $\mu\text{C}/\text{cm}^2$ , and the coercive field  $E_c$  about 0.15 kV/cm. Figure 2 (b) shows  $P_s$  vs  $T$  and  $E_c$  vs  $T$  on heating. The spontaneous polarization  $P_s$  is zero in phase-V, and increases sharply above 274.5 K with increasing temperature. It then turns to decrease continuously up to  $T_3$ , but does not vanish above  $T_3$ . The coercive field  $E_c$  is almost independent of temperature.

Figure 4 (a) shows the temperature dependence of  $\epsilon_c$  and  $\epsilon_a$  on heating between 300 K and 785 K. Dielectric anomalies appear at 561 K and 762 K, of which positions are in agreement with those assigned in neutron diffraction studies and DTA measurements<sup>5),6)</sup>. The phase transition at  $T_2$  was also observed by birefringence measurement for the  $ac$ -plate sample also performed by us. At this point thermal hysteresis of  $\epsilon_c$  was not observed in heating and cooling runs, and no latent heat was detected in our DSC measurement. However, the transition at  $T_1$  was accompanied by thermal hysteresis of about 7 K. Thus, the transitions at  $T_2$  and  $T_1$  can be recognized as second- and first-order ones, respectively

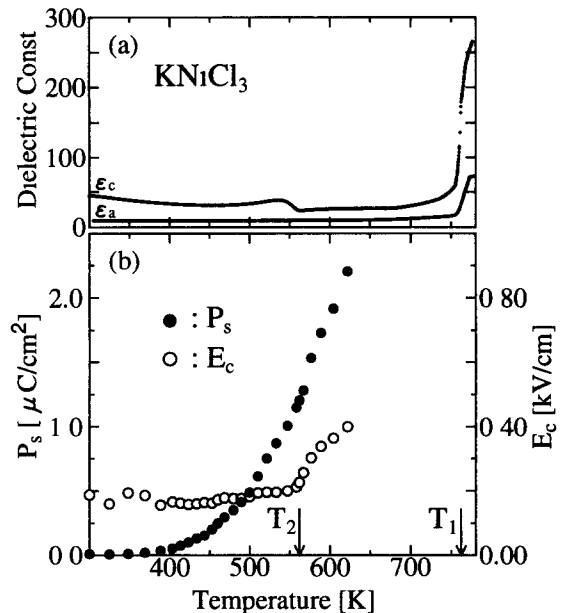


Fig 4 (a) Temperature dependence of dielectric constants  $\epsilon_c$  and  $\epsilon_a$  measured in a heating run at 1MHz above room temperature (b) Spontaneous polarization and coercive field as a function of temperature in a heating run

The imaginary part  $\epsilon_c'$  increased gradually with the increase of temperature close to  $T_2$  on heating and showed a bend at this point. Then it kept constant up to about 700 K and increased very sharply above this temperature. It was also ascertained that as the measuring frequency was reduced, the anomaly of  $\epsilon_c$  at  $T_2$  diminishes and the divergent behavior of  $\epsilon_c'$  shifts to temperatures lower than 700 K. A photograph of a  $D - E$  hysteresis loop taken at 533.0 K in phase-III is shown in Fig 3 (d). The hysteresis loops like this are observed only for the  $c$ -plate samples, and no hysteresis loops can be observed for the  $ac$ -plate samples. Figure 4 (b) shows plots of  $P_s$  and  $E_c$  with temperature extracted from the ferroelectric  $D - E$  hysteresis loops, in a temperature range from 300 K to 625 K. The magnitudes of  $P_s$  and  $E_c$  at 533.0 K were about 0.871  $\mu\text{C}/\text{cm}^2$  and 0.196 kV/cm, respectively. Because of drops in the resistance at higher temperatures ( $\sigma \sim 10^{-2} \text{ S} \cdot \text{m}^{-1}$  at 630 K), electric fields high enough to saturate the hysteresis loops could not be applied to the specimen above 600 K. However, below 600 K the hysteresis loops were confirmed to grow in the direction of saturation with the high electric field. As seen in Fig 4 (b),  $P_s$  displays no anomaly at  $T_2$  in spite of some bending in  $E_c$ , and increases monotonically as the temperature is increased through  $T_2$ . In order to examine this unexpected temperature dependence, pyroelectric-charge measurement was performed in a temperature range from 300 K to 440 K. The pyroelectric charge has a temperature dependence similar to  $P_s(T)$ . The spontaneous polarization was reversed

in sign by changing the polarity of the external electric field, and its magnitude was in good agreement with that estimated from the hysteresis loops. Furthermore, it was confirmed from the pyroelectric-charge measurement that spontaneous polarization appears in the same sense in both the high-temperature (phases-II and -III) and low-temperature (phase-IV) regions

#### § 4 DISCUSSION

$\text{KNiCl}_3$  exhibits spontaneous polarization along the  $c$ -axis in phases-II, -III and -IV, and is identified with a new ferroelectric crystal. Unfortunately, hysteresis loop observation and pyroelectric-charge measurement were quite difficult to carry out at temperatures above 630 K because of steep enhancement of electric conductivity due to ionic impurity conduction. It is most likely that the spontaneous polarization disappears at the transition from phase-II to -I. At any rate, the observed temperature dependence of  $P_s$  is anomalous, hence, the dipole arrangements in  $\text{KNiCl}_3$  responsible for  $P_s$  cannot be ferroelectric but ferrielectric. As already quoted, the structure with  $P6_3cm$  is induced from the modes with the symmetry  $K_4$ ,  $A_{2u}$  and  $K_1$  of the prototype  $P6_3/mmc$ . Since phase-II was found to be polar, the transition from phase-I to -II is interpreted adequately as a symmetry change from the space group  $P6_3/mmc$  to that of  $P6_3cm$  due to the condensation of these modes. In phase-II, whereas all  $\text{K}^+$  ions remain crystallograph-

ically equivalent,  $\text{Ni}^{2+}$  and  $\text{Cl}^-$  ions each split into two different groups. Thus two-thirds of the  $\text{NiCl}_3$ -chains have the same symmetry which is different from that of the remaining one-third. Individual displacements of respective sublattices along the  $c$ -axis, which involve antiparallel shifts of the two kinds of the  $\text{NiCl}_3$ -chains allowed by the  $K_4$ -mode symmetry, enable to establish antiparallel alignment of electric dipole moments. The competition of the moments contributes ferrielectrically to the resultant spontaneous polarization of phases-II and -III, which causes the observed temperature dependence of  $P_s$ . Since the phase transition at  $T_2$  is second order, the space group of phase-III must be a class lower than that of  $P6_3cm$ . This conjecture about phase-III is not consistent with the structural analysis by X-ray diffraction of Visser and co-workers<sup>5),6)</sup>. They remarked that at room temperature  $\text{KNiCl}_3$  was partly disordered and the hexagonal structure was found to coexist with an orthorhombic one.

At present the mechanism responsible for the temperature dependence of  $P_s$  in phase-IV is difficult to understand because we have no information on the structure below  $T_3$ . To fully understand the mechanism of the structural phase transitions including the ferroelectric phases-II, -III and -IV, a precise structural analysis over the entire temperature range is necessary.

This study was supported in part by a Grant-in-Aid for Scientific Research from the Ministry of Education, Science and Culture.

#### REFERENCES

- 1 N Achiwa J Phys Soc Jpn **27** (1969) 561
- 2 H Tanaka, Y Kaahwa, T Hasegawa, M Igarashi, S Teraoka, K Iio and K Nagata J Phys Soc Jpn **58** (1989) 2930
- 3 H Tanaka, T Hasegawa and K Nagata J Phys Soc Jpn **62** (1993) 4053
- 4 T Kato, K Iio, T Hoshino, T Mitsui and H Tanaka J Phys Soc Jpn **61** (1992) 275
- 5 D Visser, G C Verschoor and D J W Ijdo Acta Crystallogr **36** (1980) 28
- 6 D Visser and A Prodan Phys Status Solidi **A58** (1980) 481
- 7 J L Mañes, M J Tello and J M Pérez-Mato Phys Rev **B26** (1982) 250
- 8 J M Pérez-Mato, J L Mañes, M J Tello and F J Zúñiga J Phys **C14** (1981) 1121
- 9 Von H Fink and H J Seifert Acta Crystallogr **B38** (1982) 912
- 10 M Eibshutz, G R Davidson and D E Cox AIP Conf Proc **18** (1973) 386
- 11 T Kato, K Machida, T Mitsui and K Iio in preparation
- 12 T Mitsui, K Machida, T Kato and K Iio in preparation